

# Color rendering map: a graphical metric for assessment of illumination

Jesús M. Quintero,<sup>1,2</sup> Antoni Sudrià,<sup>1,4</sup> Charles E. Hunt,<sup>1,3</sup> and Josep Carreras<sup>1,\*</sup>

<sup>1</sup>*IREC, Catalonia Institute for Energy Research*

*Jardins de les dones de negre 1. PL2, 08930 Sant Adri de Bess, Barcelona, Spain*

<sup>2</sup>*Department of Electrical and Electronics Engineering, Universidad Nacional de Colombia, Bogotá, Colombia*

<sup>3</sup>*California Lighting Technology Center, University of California 633 Pea Ave, Davis California, 95618. USA*

<sup>4</sup>*Department of Electrical and Electronic Engineering, Universitat Politècnica de Catalunya, Barcelona, Spain*

[\\*jcarreras@irec.cat](mailto:jcarreras@irec.cat)

**Abstract:** The method of evaluating color rendering using a visual, graphical metric is presented. A two-dimensional Color Rendering Map (CRM) of a light source's color-rendering capabilities is explained and demonstrated. Extension of this technique to three-dimensional CRMs of objects under illumination is explained, including the method of introducing numerical indices in order to evaluate standards for specific applications in lighting. Three diverse applications, having a range from subtle to significant color variation, are shown with their respective CRMs. These three applications are also used to demonstrate how three differing light sources produce different maps. The results show a flexible, simple method to obtain a clear, visual determination of color rendering performance from differing sources used in differing illumination applications. The use of numeric indices in these applications shows how specific standards can be imposed in assessing the applicability of a light source.

© 2012 Optical Society of America

**OCIS codes:** (330.1710) Color, measurement; (330.1715) Color, rendering and metamerism; (330.1730) Colorimetry; (230.3670) Light-emitting diodes.

---

## References and links

1. CIE, "Method of specifying and measuring color rendering properties of light sources," CIE Publ.No.13.3, (Central Bureau of the CIE, Vienna, Austria, 1995).
2. CIE, "Color rendering of white LED light sources," CIE Publ.No.177, (Central Bureau of the CIE, Vienna, Austria, 1995).
3. Y. Ohno, "Color rendering and luminous efficacy of white LED spectra," Proc. SPIE **5530**, 88–98 (2004).
4. M. S. Rea and J. P. Freyssinier-Nova, "Color rendering: a tale of two metrics," Color Res. Appl. **33**, 192–202 (2007).
5. W. Davis and Y. Ohno, "Color quality scale," Opt. Eng. **49**, 033602–033616 (2010).
6. K. Smet, W.R. Ryckaert, M. R. Pointer, G. Deconinck, and P. Hanselaer, "Memory colours and colour quality evaluation of conventional and solid-state lamps," Opt. Express **18**, 26229–26244 (2010).
7. M. R. Luo, "The quality of light sources," Color. Technol. **127** 75–87 (2011).
8. P. van der Burgt and J. van Kemenade, "About color rendition of light sources: the balance between simplicity and accuracy," Color Res. Appl. **35**, 85–93 (2008).
9. D. Malacara, *Color Vision and Colorimetry Theory and Applications* (SPIE, 2002), Chap.4.
10. N. Ohta and A. R. Robertson, *Colorimetry: Fundamentals and Applications* (Wiley, 2005), Chap. 6.
11. M. D. Fairchild, *Color Appearance Models*, 2nd ed. (Wiley, 2005), Chap. 10–16.

12. X-Rite®, *The Munsell Book of Color*, Glossy Collection.
13. K. Smet and L. A. Whitehead, "Consideration of Meta-Standards for Color rendering Metrics," in *Proceedings of the 19th Color Imaging Conference*, I.S& T. Publ., (San José, CA, 2011).
14. Josep Carreras, Catalonia Institute for Energy Research, Jardins de les Dones de Negre 1. PL2, 08930 Sant Adrià de Besòs, Barcelona, Spain and Charles E. Hunt are preparing a manuscript to be called Efficacy and color rendering limits in artificial light sources emulating natural illumination.
15. J. Pérez-Carpinell, M. D. de Fez, R. Baldov and J. C. Soriano, "Familiar objects and memory color," *Color Res. Appl.* **23**, 416–427 (1998).
16. János Schanda, "Getting Color right: Improved visual matching with LED light Sources," presented at the Professional Lighting Design Convention 2011, 19-22 Oct. 2011.

## 1. Introduction

The CIE Color Rendering Index (CRI), first proposed in 1964, and later updated in 1974 [1], is the most common metric currently in use for assessment of artificial light sources in their ability to render visible colors. The Special CRI or  $R_i$ , as individual color difference index of 14 color test samples, and the General CRI, or  $R_a$ , as the index averaging the color difference of the first eight of the  $R_i$  color-test samples (all taken from the Munsell Book of Color), involve an obsolete chromatic adaptation and use a color space which is not uniform. It has been shown that these metrics incorrectly estimate the color rendering capabilities of light sources, notably white Light-Emitting Diodes (LED) [2]. There is general consensus that the General CIE-CRI ( $R_a$ ), and Special CRI ( $R_i$ ), need a re-evaluation [3].

In recent years, there have been several proposals for improving the CIE-CRI, or for establishing a different metric which evaluates a light source's color-rendering capabilities. All of these proposals can be categorized as either objective or subjective-based measures. The majority are objective-based, using a reference illuminant for comparison and intended for improving the CIE-CRI. The subjective measure proposals focus on color preference or memory colors. The following proposals are among the most recent and relevant.

The Gamut Area Index (GAI) [4] is an objective measure calculated as a percentage of the area of the polygon defined by the chromaticities in CIE-1964 coordinates of the eight CIE color test samples as specified in [1] when illuminated by a test light source, compared to the same polygon area when illuminated by a reference, equal energy white spectrum. The GAI is complementary to the CIE-CRI, and the test source is deemed both natural and vivid when both the CRI and GAI have values exceeding 80.

The Color Quality Scale (CQS) [5] is a method which mixes color fidelity and people's preference for chroma enhancement, by using more saturated test-color samples. The CQS does not penalize (nor reward) for increased chroma, includes improvements for chromatic adaptation, and uses a more homogeneous color space in evaluating color differences.

The Memory Color Rendering Index (MCRI) [6] MCRI evaluates a more subjective aspect of color rendition by calculating the degree of similarity between a set of familiar objects illuminated by the test source and their memory colors.

The proposed CRI-CAM02UCS [7] improves upon the CIE-CRI because it uses the CAM02-UCS that is not only a color appearance model but also a uniform color space, replacing the obsolete Von-Kries chromatic adaptation and the less uniform CIE 1964 ( $U^*V^*W^*$ ) space.

Among the proposals for a better, or different metric of color rendering, some focus on the test-sample set of colors (or color-order system), others use a uniform color space, others redefine the existing CIE-CRI in order to give better qualification to specific light sources, and, finally, some focus on subjective issues. Because these approaches are general metrics, none of them take into account the specific color rendering requirements constrained by particular applications. We present here, and demonstrate, a new approach, called the Color Rendering Map (CRM), which is used for evaluating and assessing light sources. The CRM is flexible

with the choice of color-order system, can work in a uniform (or non-uniform) color space, is light-source technology neutral, and can be either used as a general evaluation metric, or adapted to assess a source's value to any specific illumination application (such as artwork, food, public places, portraiture, etc.). Therefore, the CRM incorporates the useful qualities of several of other evaluation techniques which have been developed. The method produces a visual, graphical result (a map) over the chosen color space, providing more descriptive information than is possible using exclusively one or two metrics. From these representations, single number, application-dependent indices can easily be extracted when so required. Van der Burgt has also noted the need for more informative color-rendering evaluation methods [8]. However, his description is based on specifying color-shift directions plotted on the CIELab space. The CRM method is more generic in the sense that gives absolute values of rendering indices along a color space, and color rendering shifts can be easily obtained by calculating gradient plots of our data. It also has the potential to readily allow the user to evaluate a source (or compare multiple sources) specific to a particular application.

In this work, we first describe and demonstrate the use of a 2-D CRM in the process of giving a general evaluation of any light source. We then show the method to obtain a 3-D CRM of a light source to a specific application, based on the illuminated test-samples reflectance values. These 3-D representations provide immediate, intuitive information concerning the color-rendering capability that any light source has when used for that specific application. Several example applications are given to demonstrate that a lamp's color rendering can vary, according to each application. These results demonstrate an alternative to a single-number color-rendering metric.

## 2. The general Color Rendering Map of a source

We first demonstrate mapping the color rendering of a light source without any consideration of a specific application. This results in a two-dimensional CRM. Figure 1, depicts the process whereby a 2D-CRM is generated. Following the method defined in [1], established for calculation of the Special CIE-CRI (where  $R_i = 100 - 4.6 \cdot \Delta E_i$  to each one of the 14 test color samples), the evaluation of all 1269  $R_i$  values from the Munsell Book of Color is performed using the Lamp under Test, resulting in the data which is plotted in a map (the CRM), with a range encompassing all values of the data points. This results in a two-dimensional CRM. A mathematical transform has been used to avoid negative values for  $R_i$ , not altering those  $R_i$  values higher than 20. Although it is known that Munsell samples are highly correlated because are made of a limited number of pigments, Munsell set of reflectance samples is used because it is well known for the non-expert, and has a large-area gamut of colors to describe a wide range of applications, which will be useful for the 3D-CRM later on.

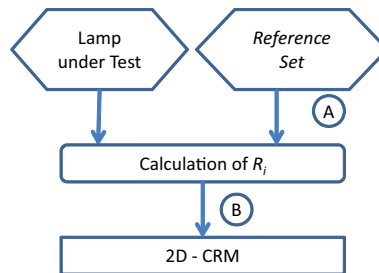


Fig. 1. Flow chart depicting how to create 2D-CRM. (A) Using the 1269 Munsell Colors, the  $R_i$  values are evaluated by comparison with a *Reference Set*. (B) The  $R_i$  values are plotted over the CIE  $x$ - $y$  plane.

As an example of this, consider the three spectra shown in Figs. 2(a)–2(c). These correspond to (a) a tri-junction R-G-B LED lamp, (b) a trichromatic fluorescent lamp, and (c) a Planckian source, band-passing the 450–650nm region of the visible spectrum. Figure 2 also lists the spectral luminous efficacy of radiation (LER) for each source, which are approximately equivalent. Although the spectra in Fig. 2 are obviously different, and render colors based on their own spectral content throughout the visible region, the CIE calculations give virtually identical  $R_a=85$  and CCTs ( $\sim 3000\text{K}$ ) for all three. This is a clear indication that these numbers by themselves provide insufficient information. The resultant danger of relying on one or two-metric evaluations is the potential to obtain a light source with spectral content mismatched to its intended application. In CIE Publication 13.3, the appearance of fifteen color samples (Special CRI or  $R_i$  for  $1 \leq i \leq 14$ ) illuminated by the light source being tested, is compared to the appearance of the same samples illuminated by a reference illuminant. The eight first differences are averaged, resulting in the General CRI ( $R_a$ ) value,  $R_a = \frac{1}{8} \sum_{i=1}^8 R_i$ . Any deficiency results in a  $R_a$  less than 100, but there is no indication in which part of the source's spectral content the deficiency lies.

To generate the 2-D CRM, the source being tested is evaluated by following exactly the same procedure as described in CIE 13.3, but substituting the 14 Munsell reflectance patterns by our *Reference (color) Set* of the entire 1269 Munsell set. The final map is obtained by plotting the entire set of  $R_i$  values over the x-y color coordinates plane, as shown in Fig. 2(d). This calculation is quickly performed from the measured spectrum of the source being tested, on the computer, using a packaged engineering environment such as Matlab. The individual  $R_i$  numbers, in this example, are graphed using colors (deep blue = 0 up to deep red = 100), resulting in the CRM figures seen next to their respective spectra, in Figs. 2(a)–2(c). The result is an intuitive, visual description of the three different sources, immediately demonstrating where are the respective strengths and deficiencies in their ability to render color, despite the fact that their  $R_a$  and CCT are identical.

It should be noted that, for purposes of demonstration, we have used the Munsell set as our reference, the CIE x-y coordinates, and color depiction of the  $R_i$  numbers within the *Reference Set*. Proposing other test samples with superior colorimetric properties or avoiding metameric correlation among test samples lies out of the scope of this work. In the following section, we present a new methodology to assess light quality of sources for a particular application.

In the demonstration examples through this paper, uniform color spaces like CIELAB and CIECAM02 are used to measure color distances, but in most cases the xyY color space is used only for graphical representation of the CRM.

### 3. The 3-D CRM and its application

The map technique described in Section 2 only gives a color-rendering description of a light source without considering the application. However, there are specific cases where color quality is of highest importance, and where the careful selection of a suitable spectral content is critical. In such specific situations, general indices are not a valid option.

We present in this section a methodology for assessment of the color quality of light sources under a particular application. As inputs, this method requires not only the spectrum of the light source, but also the chromaticity coordinates of all the illuminated elements (i.e. image pixels obtained with a luminance/color camera) under a reference illuminant (in our case, a D65 simulator). We use a Class B, (which is in the limit of being Class A since the measured Metameric Index is  $MI_{vis}=0.268$  (under CIE-L\*a\*b\*) and  $MI_{vis}=0.328$  (under CIE-L\*u\*v\*)), which has enough resemblance to the D65 CIE standard illuminant for our purposes, since the minimum distance between consecutive samples of the Munsell set is  $\Delta E_{Lab}=4.86$ .

For a particular application (i.e. artwork, food, retail, etc.) we use a 3D representation of

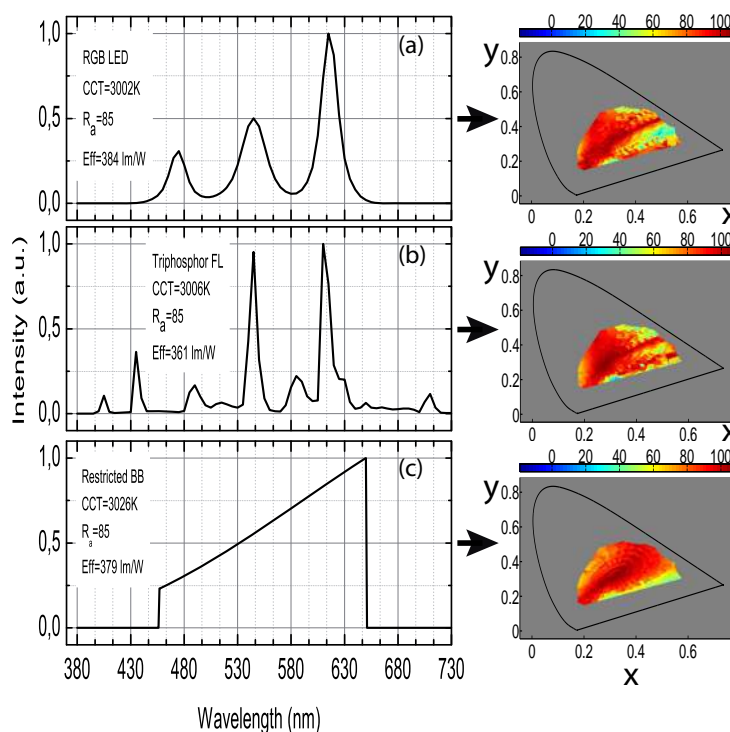


Fig. 2. Three differing CCT=3000K spectra, (a) white R-G-B LED, (b) trichromatic fluorescent, and (c) filtered Plankian, all having the same CRI ( $R_a$ ) values and approximately identical LER values. The Color Rendering Maps (CRMs) are depicted next to their respective spectra.

the color coordinates obtained with the luminance camera. This is performed by using different color spaces, such as CIE 1931 xyY [9], the CIE 1976  $L^*a^*b^*$  (CIELAB) [10], and the CIECAM02 [11], each of these having increasing complexity and computational power demands.

In order to evaluate how a light source renders the whole set of colors present in a particular application, the process followed is to first choose an ordered set of colors based on a color order system, resulting in what we call a *Reference Set*. The color coordinates of the object of interest in the application are then measured with the luminance camera (which incorporates filters emulating the  $2^\circ$  observer matching functions,  $\hat{x}$ ,  $\hat{y}$  and  $\hat{z}$  as illuminated by our D65 simulator, the resulting set of color coordinates being what is called the *Observed Gamut*. Again, although filters incorporated in these cameras are not perfect matches to the CIE matching functions, the x-y error is less than  $\Delta E < 2 \cdot 10^{-3}$  under A CIE standard illuminant. Finally, a sub-set of the *Reference Set* is selected by finding minimum distances between the *Observed Gamut* and the *Reference Set*, resulting in the *Test Set*. This *Test Set* is then mapped in the 3-D color space chosen, creating the CRM. The flow chart in Fig. 3 depicts this process. There is also available an online animation depicting the whole CRM build-up process, see Fig. 3 ([Media 1](#) and [Media 2](#)).

The *Reference Set* requires a group of test colors of a sufficiently wide range of hue, chroma and lightness, such that this set contains all the colors present in all the objects associated with application of interest. For purposes of the examples which follow, we use a reflectance

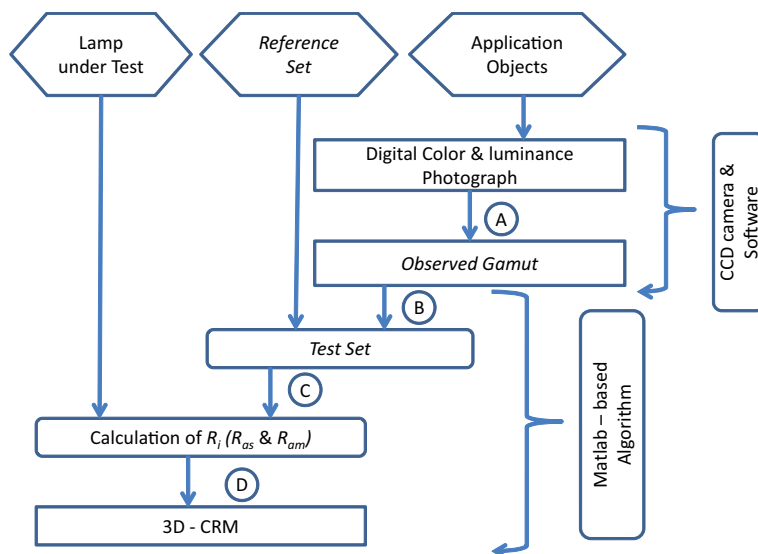


Fig. 3. Flow chart for the evaluation of the 3-D CRM. (A) A calibrated digital photograph measures all luminance and color coordinates of the application object, giving the *Observed Gamut*. (B) The *Test Set* is obtained by finding the closest Euclidian distance between each pixel in the Measured Set to the Colors of the *Reference Set*. (C) As before, the  $R_i$  values for the complete *Test Set* (as well as the  $R_{as}$  and  $R_{am}$  indices) are computed. (D) Finally, the 3-D CRM is plotted using the  $R_i$  values of the Test Sample [Animation available online. Low Bit-Rate (low weight): [Media 1](#). High Bit-Rate (high weight): [Media 2](#)].

database of the 1269 color samples corresponding to the Munsell color system, as was used in Section 2. This *Reference Set* is 90% of the color samples of the Munsell Book of Color (used for color assessment in industrial applications [12]), and although it demonstrates some metameric weaknesses, it suffices to demonstrate the CRM in the cases we tested. Other authors have demonstrated good color appearance modeling using 1000 reference colors [7], and reasonable improvement (as compared with  $R_a$ ) with as few as 17 reference colors [13].

Test objects which have a very limited gamut, or require illumination at very-low CCT values may fall not be properly mapped using the Munsell set. In such cases, a *Reference Set* drawn from a different color ordering system, such as the NCS or OSA Uniform Color Scale (depending on the objects and illumination conditions) will likely be needed to generate an accurate CRM.

Using a digital luminance camera, we obtain a picture of the test objects illuminated by our D65 simulator. It is necessary to calibrate the color and luminance of the camera using a standard illuminant, and include (during the test) a test card of a range of the reference colors to verify the accuracy. Editing the area(s) of interest of the picture, removing any test cards or surfaces of the experimental viewing booth from consideration in the data, the set of pixels that represent the chromaticity of the test objects are obtained (*Observed Gamut*). Subsets of these areas of interest can also be examined, which may give rise to a slightly different *Observed Gamut*, depending on the diversity of colors in the test objects of the application. While this variability might be seen as a weakness of the method, it actually emphasizes the high level of customization that it is able to provide, assessing color rendering aimed at each special case. In those applications where the diversity of colors is extremely broad, the benefits of our CRM are not so clearly seen, and other metrics that only depend on the spectrum of the light source but not on the input gamut might make more sense.



The *Observed Gamut* is compared to the *Reference Set*, resulting in a sub-set (of the *Reference Set*) which is the *Test Set* that represents the color gamut of the objects. This comparison is performed between each single pixel of the *Observed Gamut* to all samples of the *Reference Set* and assigning to the *Test Set* the nearest color within a uniform color space (such as CIELAB or CIECAM02). Colors in the *Observed Gamut* can occur multiple times, which is noted using a multiplicity factor,  $m_i$ , with a integer value  $m_i \geq 1$ , for each element in the *Test Set*. The *Test Set*, along with the respective  $m_i$  values, allows us to create the 3-D Color Rendering Map and two associated numerical indices as seen in Eqs. (1) and (2). These indices are used for color-rendering evaluation of the test light source; but are specific to the application being studied, and are not intended as a replacement or substitute for the CIE- $R_a$ , but as a complement for those applications for which color must be accurately controlled. It is evident that the value of multiplicity is highly dependent both on the diversity of color in the test objects, as well as to the size of the area of interest chosen from which to draw the *Observed Gamut*. The user of the CRM chooses, according to his requirements, the value of  $R_{as}$  and/or  $R_{am}$  which can be considered acceptable for the application being studied.

Once the *Test Set* is defined, and using the spectrum of the Lamp under Test (see stage C in Fig. 3), the average of all  $R_i$  values, as defined in [1], of this set is the index  $R_{as}$ . Considering that some samples have greater weight, if their  $m_i \gg 1$  (a likely situation in most applications) in the gamut, the color rendering is also calculated as a weighted index,  $R_{am}$ . The sum of all pixels in the *Observed Gamut*, given their respective  $m_i$  values is evaluated as:

$$R_{as} = \frac{1}{s} \sum_{i=1}^s R_i \quad (1)$$

$$R_{am} = \frac{1}{u} \sum_{i=1}^s m_i \cdot R_i \quad (2)$$

$$u = \sum_{i=1}^s m_i \quad (3)$$

Where:

$s$ : Number of elements in the *Test Set*.

$u$ : Number of elements (pixels) of the *Observed Gamut*.

$m_i$ : Multiplicity of the  $i$ -th element in the *Test Set*.

It is important to note that the index values vary for a single light source, since the *Test Set* changes with differing applications. Therefore,  $R_{am}$  and  $R_{as}$  cannot serve to replace general CRI,  $R_a$ , but are application specific. Because an end user selects the area of interest to assess, even within a particular application, a given light source can produce differing indices if the user places attention on differing areas of interest. However, in general, the index value will become of lesser utility for smaller areas. Furthermore, we have not included issues of metamerism in these indices, and in some applications those conditions need to be addressed.

Considering that human vision has adapted to natural daylight, an artificial light source is perceived as natural if it emulates a Planckian radiator [14]. By this standard, color quality can be objectively measured by considering parameters such as the Correlated Color Temperature (CCT) and the deviation of the chromaticity coordinates from the black body locus ( $\Delta_{uv}$ ) in addition to its  $R_a$  value. However, color quality assessment in general lighting sources has some subjective components such as color preference, memory colors and other issues varying with individuals [15]. The selection of areas of interest is already a subjective process reflected by the *Observed Gamut*; however, this is unique to each application, and defined by the user. Furthermore, although objective measurements can find the chromaticity of a source based on

the spectral power distribution, the phenomena of metamerism, where two sources with the same chromatic coordinates (but different spectral content) generate different color perception of some objects [16], would have to be evaluated using a metamerism index for a more complete assessment of the color quality. Such subjective measures can be included in mapping an *Observed Gamut* by using methods which have been proposed by others who have described these phenomena, and how to evaluate them; but this is beyond the scope of this work which focuses on using the CRM for visual mapping of color rendering. Also, efficacy of a light source, which is of paramount importance, often has a significant, measureable tradeoff with color quality [14], and a user's threshold efficiency constraints can be incorporated into a CRM by plotting only the final data values which meet or exceed whatever value is chosen. The standards of how natural, efficient, metameric, or other qualities, as they would be incorporated in a CRM, are not addressed in the following application examples, and are reserved for future work.

#### 4. Application examples

The tools used to complete the measurement, shown in Fig. 4, include a viewing booth, both for calibration and for illumination of the objects by the chosen test sources, a CCD camera (calibrated for color and luminance), both color and gray checker cards, and software for data management and graphical representation. With these tools we are able to obtain an *Observed Gamut* for each application, and compute the *Test Set*, as well as portray the CRM.

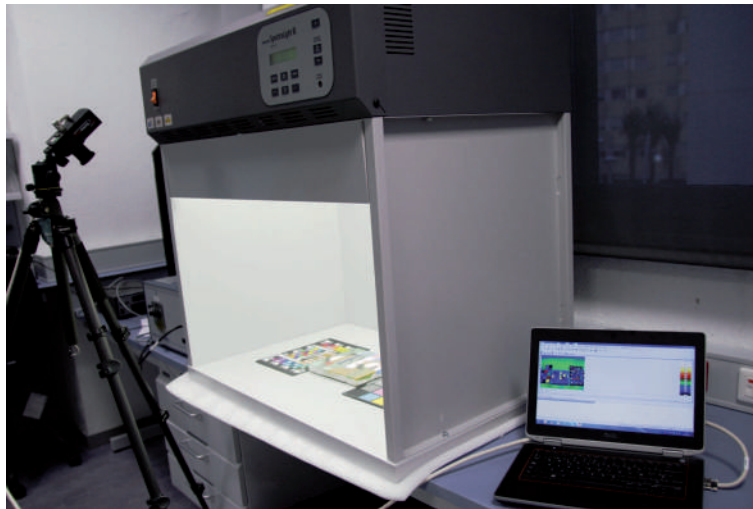


Fig. 4. Experimental viewing booth, for generating *Test Sets*, with a simulator of the standard illuminant CIE-D65, calibrated CCD camera and a computer for editing and selecting the areas of interest. Also seen in the booth are color-checker patches. All measurements are performed with room lights dark.

To assure the color and luminance calibration of the camera/software, in the test setup of Fig. 4, a color-checker card is placed in the same scene of the objects under test in the viewing booth. Test measurements are performed with ambient room lights dark. Each photograph is edited, by selecting the areas of interest, and then grouping these areas, exporting the data with CIE-1931 xyY identifiers.

Demonstrating the 1269 Munsell samples of our chosen *Reference Set* in 3-D is seen in Fig. 5, in ( the non-uniform) CIE-1931 xyY color space (a) as well as uniform CIELAB (b) and



CIECAM02 (c) color space. Figures 5(a)–5(c) show, in each case, two differing angles of view of the color coordinates of the *Reference Set*. These data, which include the luminance values, represent the 3-D analogue of the 2-D *Reference Set* shown in Fig. 2(d).

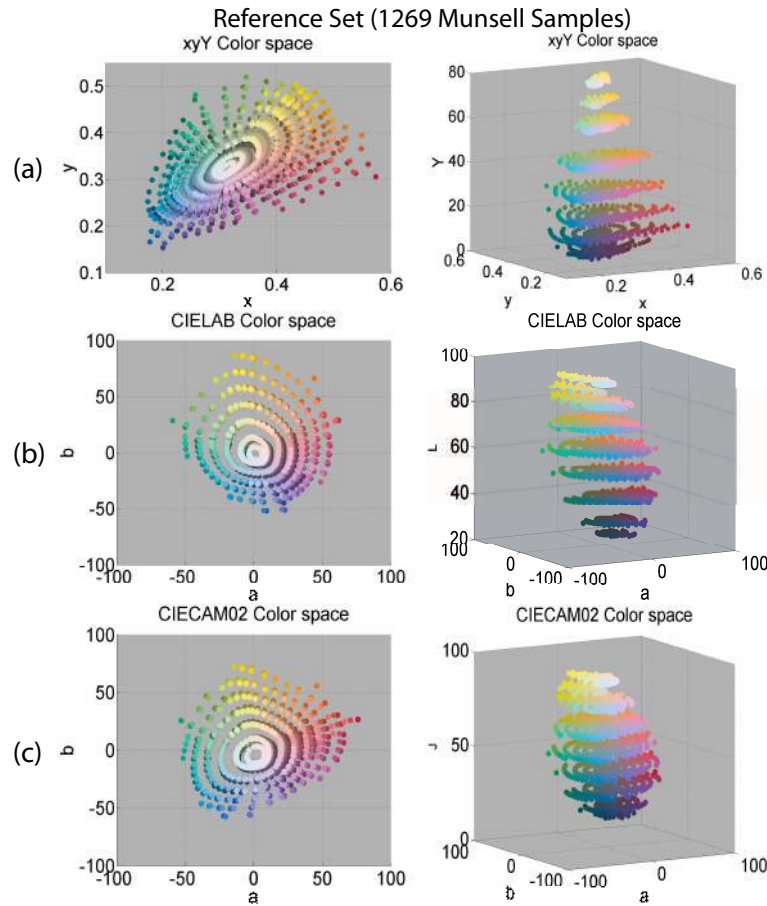


Fig. 5. 3-D color space depiction of the 1269 color *Reference Set*, analogous to 2-D representation of Figure 2d, as used in the application examples. These are seen in two views: Azimuth = 0, Elevation = 90 (left column) and Azimuth = -30, Elevation = 10 (right column). The equivalent *Reference Set* is demonstrated in three versions of color space: (a) CIE-1931 xyY, (b) CIE-1976 CIE  $L^*a^*b^*$ , and (c) CIECAM02.

Three diverse, practical lighting applications here demonstrate the CRM, seen in Figs. 6(a)–6(c) using our D65 simulator. The first case, lighting of meat in displays, seen in Fig. 6(a), examines a lighting application where the illuminated object has somewhat subtle color variations. The second, a collection of various fruits, Fig. 6(b), looks at a broader range of colors. Finally, Fig. 6(c), lighting of artwork, covers a most-diverse usage of colorfulness, saturation and lightness. For these three applications, we follow the method described in Section 3, determining the *Test Set* and evaluating  $R_{as}$  and  $R_{am}$  indices with differing light sources. Finally, we show the CRMs for each case. Table 1 shows some figures for *Observed Gamut* (pixels) and *Test Set* (selected Munsell samples) obtained for the three applications in Fig. 6.

Table 1 highlights that the color differences (in our case, using the Munsell color samples) between *Test Sets* obtained using CIELAB and CIECAM02 for these three chosen applications

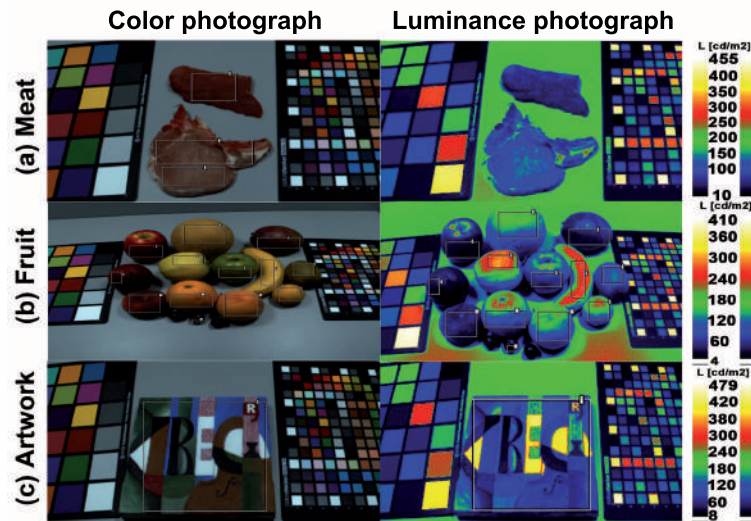


Fig. 6. Color photograph (left column), taken under a D65 CIE standard illuminant simulator, of meat samples (a), assorted fruit (b) and artwork (c), along with corresponding luminance photographs of each scene (right column). The rectangles delineate the areas of interest to be analyzed. The color-checker cards are used to verify the calibration of the camera.

Table 1. Comparative Results of Calculated *Observed Gamut* and *Test Set* using CIELAB and CIECAM02 Color Systems for Three Different Applications.

Application	Color system	<i>Observed Gamut</i> (pixels)	<i>Test Set</i> (Selected Munsell Samples)	Average Multiplicity
Meat	CIELAB	29.401	231	127
	CIECAM02	29.401	232	127
Fruit	CIELAB	134.207	170	789
	CIECAM02	134.207	174	771
Artwork	CIELAB	194.208	611	318
	CIECAM02	194.208	610	318

is negligible.

The size of any *Observed Gamut* may comprise several mega-pixels, varying on how many, and how large, the selected areas of interest are. Therefore, an algorithm that extracts the volume surface of the *Observed Gamut*, is used to optimize data management for the CRM to be represented in a 3-D graphics.

The resulting *Test Set* (solely for the meat application), is shown in Figs. 7(a)–7(c), as derived from the measurements of the application in Fig. 6(a). The *Test Sets* of Figs. 7(a)–7(c) show the two different angles of view depicted in Figs. 7(a)–7(c) for the CIE-1931 xyY, CIELAB and CIECAM02 color spaces.

The *Test Set* for each application is obtained by evaluating the minimum Euclidean distances from each single pixel of the *Observed Gamut* to each element of the *Reference Set* (i.e. the closest Munsell sample to that pixel), in these cases using the cylindrical coordinates in CIELAB and CIECAM02. Figure 8 shows the 3-D xyY *Test Set* for the three example applications as seen in Figs. 6(a)–6(c).

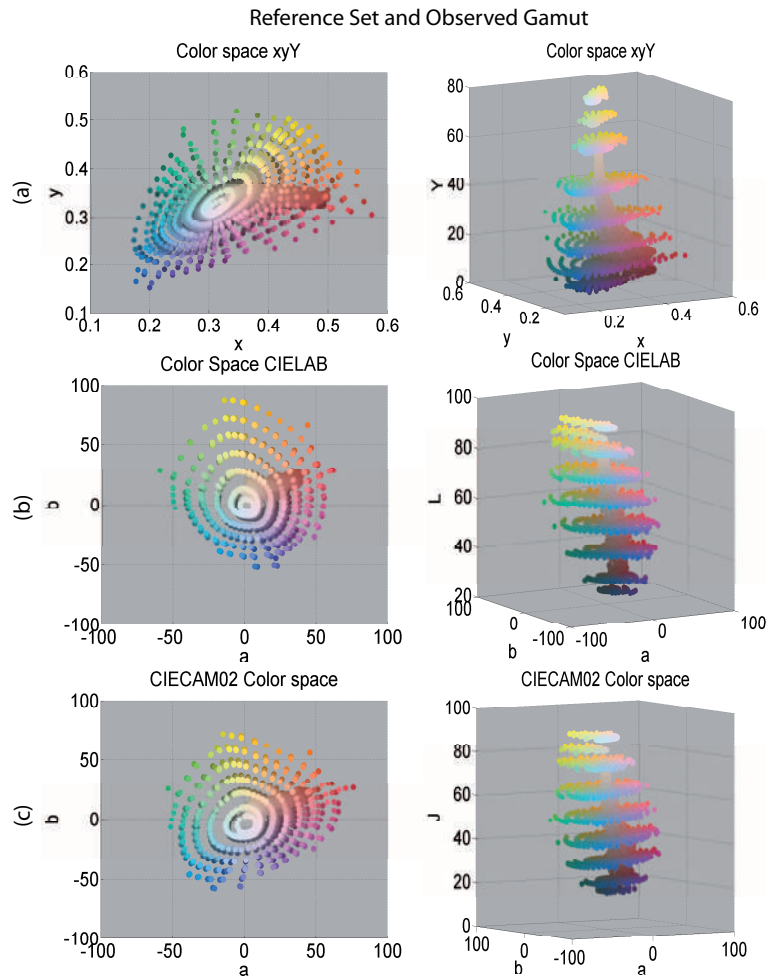


Fig. 7. *Observed Gamut* data measured under a D65 simulator from the meat application shown in Fig. 6(a), in three versions of color space: CIE-1931 xyY (a), CIE-1976 L\*a\*b\* (b) and CIECAM02 (c). These are seen in two views: Azimuth = 0, Elevation = 90 (left column) and approximately Azimuth = -30, Elevation = 10 (right column)

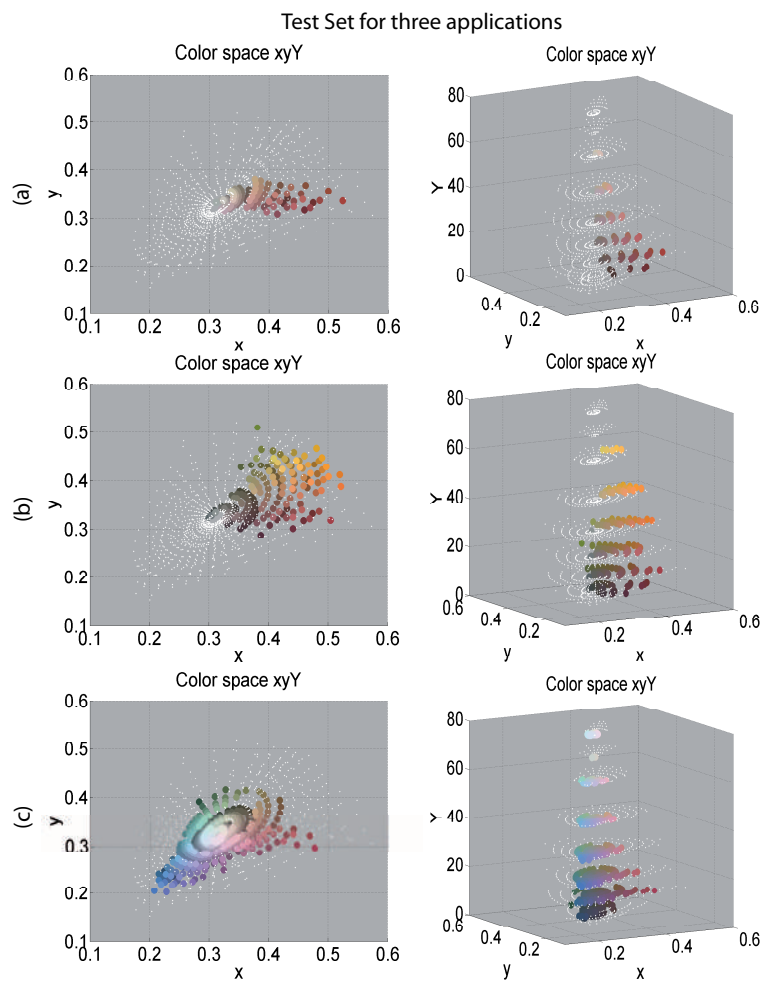


Fig. 8.  $xyY$  representation of the *Test Set* found for the meat (a), fruit (b) and artwork (c) applications of Fig. 6.

We now analyze three different light sources (with comparable CCT's and  $R_a$ 's) as shown in Fig. 9 (left) by following the steps described above for the calculation of the *Test Set* and for the indices  $R_{as}$  and  $R_{am}$ . It can be seen (Fig. 9, left) that even though the  $R_a$  value remains essentially the same for each light source (and strictly the same for each application because it only depends on the spectral content of the light source), the  $R_{as}$  and  $R_{am}$  indices change from application to application. This demonstrates how the CRM and the derived indices constitute a useful tool for the lighting designer when personalizing scenes in specific applications. When high color rendering is of importance (i.e. retail, artwork, surgery, etc.), the use of customized indices such as  $R_{as}$  and  $R_{am}$  enables the user to establish specific threshold constraints which need to be met.

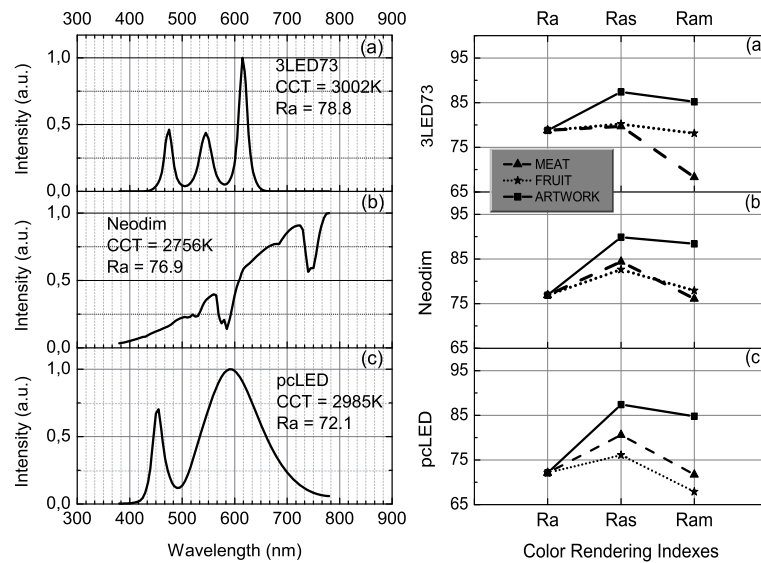


Fig. 9. Left column: Three differing light sources, CCT=3000K, (a) R-G-B LED, (b) incandescent Neodimium lamp, and (c) Phosphor-converted LED. Right column: Corresponding color rendering indices CIE- $R_a$ ,  $R_{as}$  and  $R_{am}$ , for the three applications (*Test Set*) Meat, Fruit and Artwork.

For the lamps studied in Fig. 9, the highest values of  $R_{as}$  and  $R_{am}$  are obtained for the artwork application, since artwork shows a *Test Set* with the widest range of hues.

Beyond the single-number indices  $R_{as}$  and  $R_{am}$ , a full description of the situation can be found in the next 3 figures, where the 3D-CRM has been evaluated and is shown for the different applications, i.e. meat (Fig. 10), fruit (Fig. 11), and artwork (Fig. 12).

Finally, by extracting the left column of Figs. 10–12 and the  $R_{am}$  values from Fig. 9, we obtain Fig. 13, which is a useful in assessing the suitability of the three light sources for three different applications. Although each sub-plot in Fig. 13 shows just one angle of view of the 3D-CRM, this graphical representation along with the single-number  $R_{am}$  index, gives both intuitive (visual) and quantitative information. Our combined representation comes in handy when comparing the color rendering capabilities of different light sources for a specific application, or the suitability of a light source for different applications.

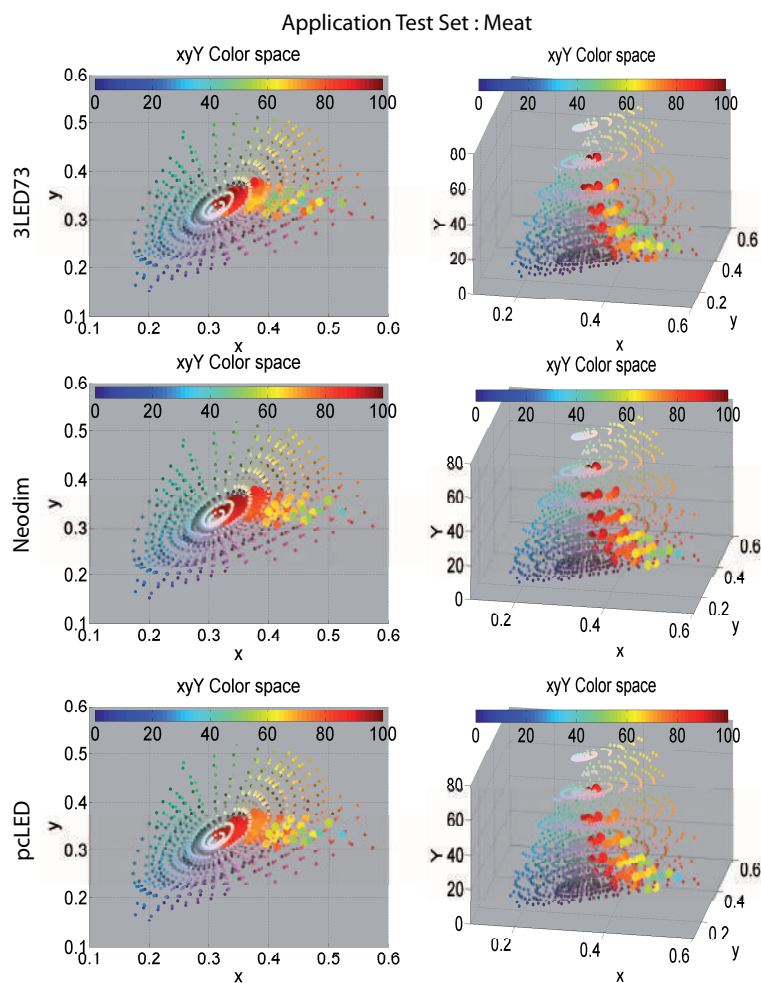


Fig. 10. CRM representation in xyY color space of the *Test Set* found for the meat application of Fig. 6, and illuminated with the light sources of Fig. 9. R-G-B LED (upper row), Neodimium (middle row) and phosphor-converted LED (lower row). These are seen in two views: Azimuth = 0, Elevation = 90 (left column) and Azimuth = 10, Elevation = 24 (right column).



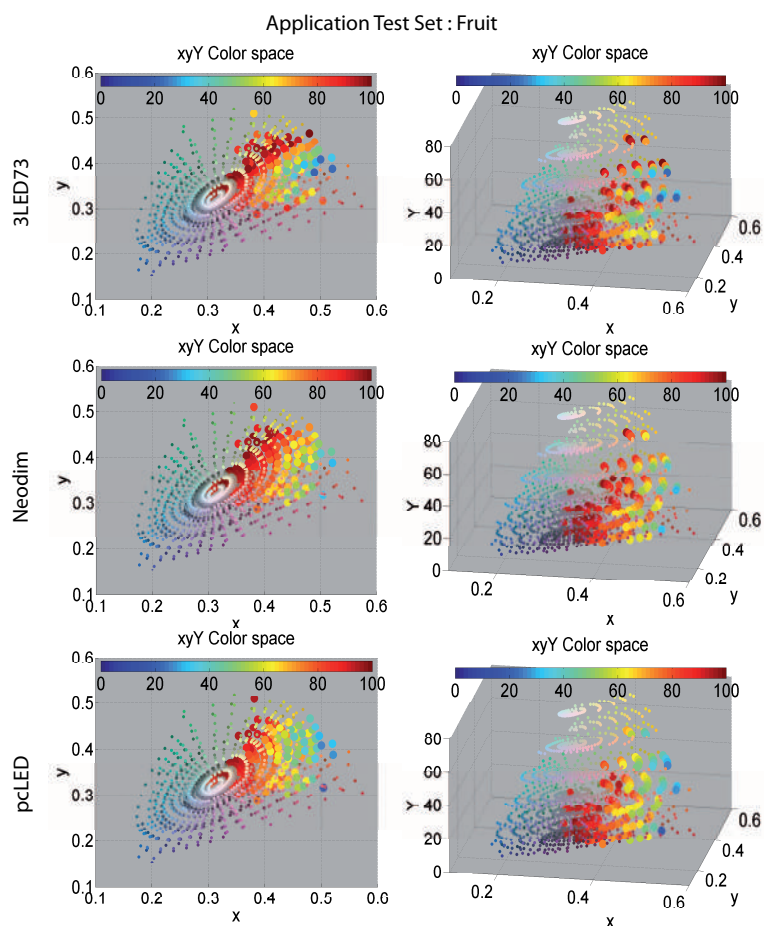


Fig. 11. CRM representation in xyY color space of the *Test Set* found for the fruit application of Fig. 6, and illuminated with the light sources of the Fig. 9. R-G-B LED (upper row), Neodimium (middle row) and phosphor-converted LED (lower row). The same views as in Fig. 10 are shown.

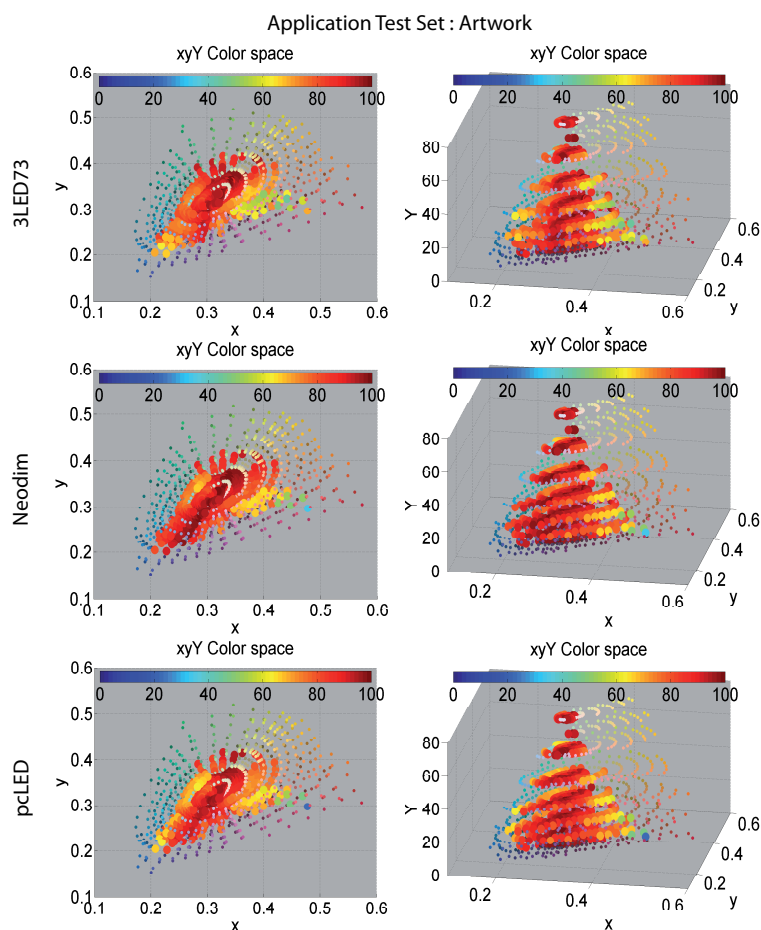


Fig. 12. CRM representation in  $xyY$  color space of the *Test Set* found for the artwork application of Fig. 6, and illuminated with light sources of the Fig. 9. R-G-B LED (upper row), Neodimium (middle row) and phosphor-converted LED (lower row). The same views as in Fig. 10 are shown.

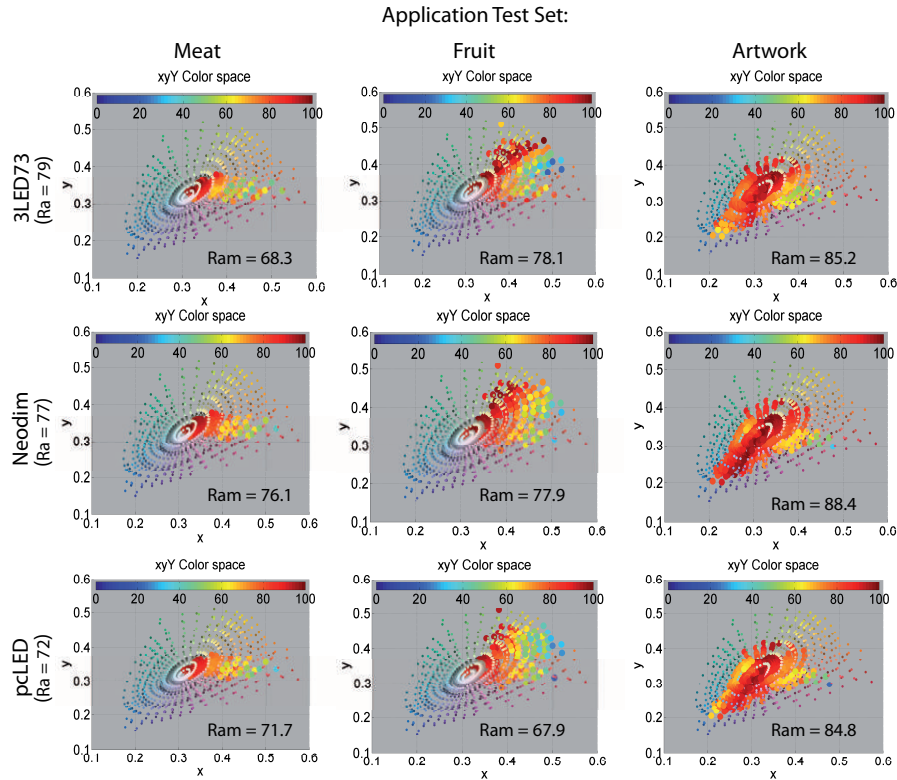


Fig. 13. CRM representation in xyY color space of the *Test Set* for the three applications shown in Fig. 6, illuminated with light sources of Fig. 9. R-G-B LED (upper row), Neodimium (middle row) and phosphor-converted LED (lower row). Only one view is shown.

## 5. Discussion

With the advent of SSL and other new technologies to come (Quantum Dots, Nano-wires, OLEDs, etc.), a great revolution in the lighting industry is underway. This is not only due to their promised energy efficiency, but also because they offer us the flexibility to make spectral matching and tuned color reproduction a reality. In the same way the lighting designer evaluates the position of the luminaires based on the desired illuminance and luminance levels of surfaces, another factor now comes into play: the color rendering of special or specific regions.

The CRM presented in this work constitutes a first attempt to develop a complete methodology that takes as an input not only the spectrum of the light source but also the color coordinates of the pixels of the scene involved, making it possible to find the best spectral content in illuminating different applications.

In the process of evaluating light sources, the 2-D CRM shows the user or lighting designer not only average, or weighted average of color rendering, but also, as is readily seen in Fig. 2, where the various deficiencies lie in the spectral content of any given light source. The CRMs of Figs. 2(a)–2(b) show clearly the expected red weaknesses in tri-junction LED lamps and trichromatic fluorescent sources. The restricted blackbody spectrum of Fig. 2(c), which is cut off at 450 and 650nm, has its saturated blue and red deficiencies immediately evident in the CRM. For a user who knows what part(s) of color space are important to a specific application, a 2-D CRM of any light source will immediately verify the applicability.

The 3-D CRM similarly allows a user to identify the areas of utility of color space, as well as lightness (volumes) within an application. Figures 10, 11 and 12 make the differences in the three demonstrated applications clear, not only in chromaticity and luminance; but also in diversity of color. This can be important if further metrics, such as efficacy or metamerism need to be considered in selecting a lamp for a chosen application: As we have seen, different light sources can have differing weak points, in luminous efficacy of radiation, over their spectral output. This inclusion of multiple metrics, and the level of sophistication required in the lighting design, become the indicators of what level of color appearance model (ie. simple, such as CIE-1931 xyY, versus complex, such as CIECAM02) ought to be employed in generating specific CRMs.

Also, although the Munsell gamut was used in this demonstration of the CRM, as the *Reference Set*, as well as the three well-known CIE color models, there is broad flexibility to expand or contract these, according the type of mapping which is desired. A *Reference Set* can range from a few hundreds of sample colors to a sophisticated color ordering system, such as the NCS or the OSA Uniform Color Scale, for a range of applications from illuminating highways to specialty lighting, such as used in medicine or cinematography. Also, a broad range of color appearance models, which also vary significantly in sophistication and power, can be used, as has been demonstrated here.

## 6. Conclusion

A method for evaluating light sources, and also for evaluating (and/or comparing) that source's desirability in specific applications using a graphical metric, the Color Rendering Map, has been described and demonstrated. A systematic method for evaluating light sources, regardless of application, has been shown using the 2-D CRM. The method of extending the evaluation to specific applications of any source has been described by using the 3-D CRM.

Solid State Lighting and the forthcoming emerging technologies will allow spectral reproduction in the near future. At that point, the Lighting Designer will be challenged by a situation in which the spectral content of a light will have to be adapted to its intended final application or space location. With this perspective in mind, the CRM constitutes an excellent tool for expanding illuminance and luminance-based designs to include color-based designs in the future.

The value of these methods is seen in their visual, graphical depiction in a map, as opposed to less descriptive, and potentially ambiguous, numeric metrics. The CRM also allows considerable flexibility in its implementation, both in limiting or expanding the palate of colors over which the user wishes to consider, or in limiting/expanding the color space for the graphical mapping.

## Acknowledgments

The research was partially supported by the European Regional Development Funds (ERDF, "FEDER Programa Competitivitat de Catalunya 2007-2013"). JC acknowledges support from the SILENCE<sup>2</sup> (TEC2010-17472) from the Spanish Ministry of Science and Innovation (MICINN). The research was also partially supported by the European project LED4Art (CIP-IST-PSP-Call 5-2010, Contract No. 297262). The authors gratefully acknowledge Mireia Nogueras for designing the artwork required for this presentation.